

# Cooling and amplifying motion of a diamond resonator with a microscope

Harishankar Jayakumar,<sup>1,\*</sup> Behzad Khanaliloo,<sup>1,\*</sup> David P. Lake,<sup>1</sup> and Paul E. Barclay<sup>1,†</sup>

<sup>1</sup>*Institute for Quantum Science and Technology, University of Calgary, Calgary, AB, T2N 1N4, Canada*

(Dated: Compiled October 11, 2024)

Controlling the dynamics of mechanical resonators is central to many quantum science and metrology applications. Optomechanical control of diamond resonators is attractive owing to diamond's excellent physical properties and its ability to host electronic spins that can be coherently coupled to mechanical motion. Using a confocal microscope, we demonstrate tunable amplification and damping of a diamond nanomechanical resonator's motion. Observation of both normal mode cooling from room temperature to 80K, and amplification into self-oscillations with 60  $\mu$ W of optical power is observed via waveguide optomechanical readout. This system is promising for quantum spin-optomechanics, as it is predicted to enable optical control of stress-spin coupling with rates of  $\sim 1$  MHz (100 THz) to ground (excited) states of diamond nitrogen vacancy centers.

The interaction between light and mechanical systems underlies breakthroughs in physics ranging from optical tweezers [1] to gravitational wave detection [2]. Nanoscale optomechanical system that harness this interaction have led to milestone advances in quantum nanomechanics [3–9], sensing [10–13], and nonlinear optics [14–18]. An essential ingredient in many of these demonstrations is dynamic optomechanical back action, in which the optical force lags the motion of the mechanical resonator, allowing energy to be exchanged between optical and mechanical domains [19, 20]. Controlling diamond based nanomechanical systems via optomechanical back action is of growing interest, fueled in part by applications that would benefit from diamond's exceptional mechanical and optical properties [21], and by recent demonstrations of control of color center electron spins using piezoelectronic driven mechanical resonators [22–30]. Excitation of mechanical motion using optomechanical back action provides a path towards optomechanical spin manipulation and photon-phonon-spin coupling, for quantum information processing technologies ranging from spin-spin coupling [31, 32] to quantum transduction [33]. This control can also be used to enhance the sensitivity and versatility of diamond resonators used in sensing applications [34–36]. In this Letter, we show that dynamic optomechanical back action acting on a diamond nanomechanical resonator can be created and tuned using the gradient of a laser focused by a microscope commonly used for diamond colour center imaging. Using this technique, we optomechanically cool a diamond nanomechanical resonator, as well as amplify its motion sufficiently to allow optomechanical control of diamond spins via their predicted coupling to phonons.

Optomechanical damping and amplification of nanomechanical structures, for example by optical gradient [37], radiation pressure [4, 38, 39], or photothermal forces [35, 40–44], typically relies on feedback created by an optical cavity [19, 20], waveguide coupler [44], or external optoelectronics [45]. The optomechanical system introduced here combines attributes of optical tweezers with delayed feedback required for optome-

chanical damping and anti-damping. It does not require a cavity or rely on coupling to optical modes of the diamond nanostructure, allows both the strength and the sign of the optomechanical damping to be tuned, and provides a desirable combination of simplicity and sensitive independent mechanical readout via an evanescently coupled fiber taper waveguide [44]. The optomechanical backaction in this system, which is photothermal in nature, is tuned through translation of a microscope focus while operating at a fixed wavelength, not requiring a wavelength dependent optical response used in previous studies of nanowire photothermal optomechanics [43]. Operating in this optical intensity gradient dominated regime of photothermal optomechanics, we perform normal-mode cooling of a diamond nanobeam mechanical resonator from room temperature to  $\sim 80$  K, and excite nanomechanical self-oscillations whose dynamical stress field is predicted to be sufficiently strong to drive the spin transitions of NV centers [22]. We show that these self-oscillations can be excited with 60  $\mu$ W of external laser power when the nanobeam is cryogenically pre-cooled to 5 K, and that in these conditions both vertical and horizontal nanobeam modes can be selectively excited.

The optomechanical system studied here, illustrated in Fig. 1(a), consists of a doubly clamped diamond nanobeam (dimensions  $l \times w \times t = 50 \times 0.5 \times 0.25 \mu\text{m}^3$ ) located within the focus of a green (532 nm) laser source input to a microscope objective (Sumitomo long working distance, 0.55 NA) mounted on a three-axis piezo stage. The nanobeam is fabricated from a single crystal diamond chip (Element Six, optical grade,  $3 \times 3 \text{ mm}^2$  area, polished by Delaware Diamond Knives) using quasi-isotropic undercut etching [44], and its top surface is coated with a thin layer of titanium ( $\sim 5$  nm thickness, deposited using electron beam evaporation), which serves the dual purpose of improving SEM image quality and enhancing photothermal effects discussed in this Letter. This fabrication process results in a monolithic diamond nanobeam suspended approximately  $2 \mu\text{m}$  above the diamond substrate, as shown in the SEM image of a typical

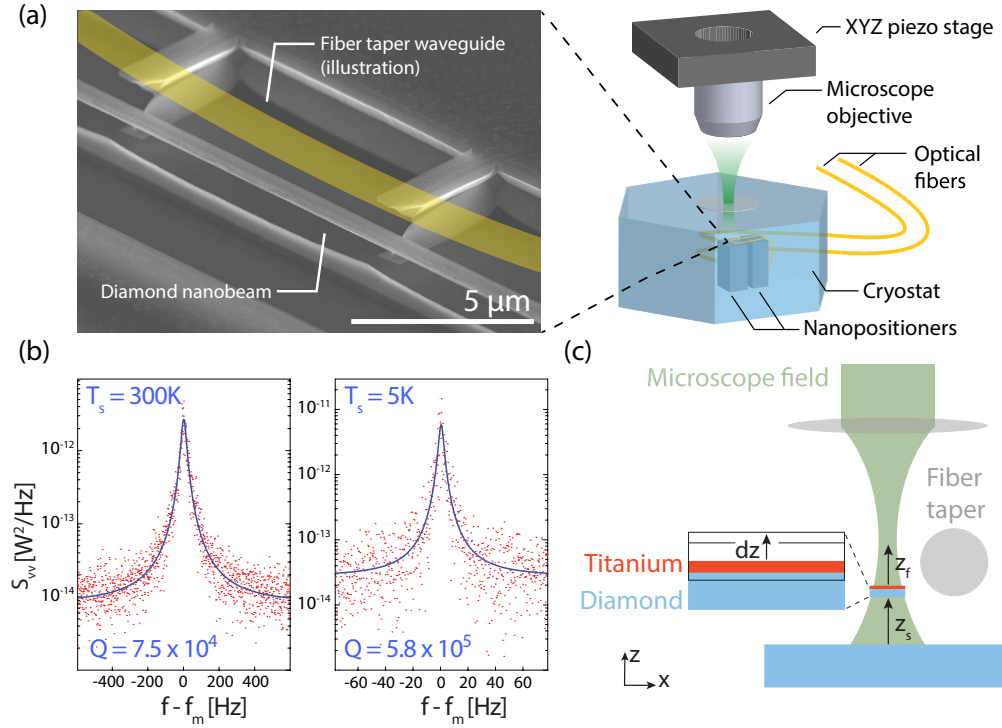


FIG. 1. (a) Schematic of the optomechanical system and measurement apparatus. A microscope objective mounted on a three axis piezo stage focuses a green laser onto the diamond sample. The sample and fiber taper are located in a cryostat on nanopositioners. SEM image: a diamond nanobeam similar to that used in the experiment, with an illustration of the dimpled optical fiber taper drawn in yellow and superimposed on the image in approximately the position used for evanescent coupling to the nanobeam. Also visible are diamond supports used to stabilize the fiber taper during measurements. (b) Power spectral density of the fiber taper transmission near the  $\mathbf{v}_1$  nanobeam mode frequency at room and low temperature. (c) Schematic of the geometry of the optomechanical system.

device in Fig. 1(a).

In the results presented below, we show that by adjusting the microscope focal spot position, the dynamics of the nanobeam's mechanical motion can be controlled e.g., amplified into self-oscillation or damped to a lower effective temperature. These dynamics are independently monitored using a dimpled optical fiber taper waveguide (diameter  $\sim 1 \mu\text{m}$ ) [46] evanescently coupled to the nanobeam, as illustrated schematically in the SEM image in Fig. 1(a). The fiber taper and the diamond sample are mounted in a closed cycle cryostat (Montana Instruments) that allows measurements to be performed in vacuum over temperatures ranging from 5K to 300K, and are aligned using nanopositioners (Attocube). Mechanical motion of the nanobeam is monitored with up to  $\text{fm}/\sqrt{\text{Hz}}$  displacement sensitivity by measuring the transduced fluctuations in the coupling ratio between the fiber taper and the nanobeam, as described in Ref. [44]. Dynamics of the nanobeam resonances are measured by recording the power spectral density  $S_{vv}$  of the photodetected transmission of a 1570 nm source through the fiber taper.

Characterization of the fundamental nanobeam verti-

cal mechanical mode (labeled  $\mathbf{v}_1$ ) in absence of the microscope field follows previous work [44], and is shown in Fig. 1(b), which plots  $S_{vv}$  over the frequency ( $f$ ) range spanning the resonance frequency  $f_m$ , in high vacuum ( $< 10^{-5}$  Torr) at 300K and 5K operating temperatures. These measurements show a peak in  $S_{vv}$  corresponding to the thermally driven motion of  $\mathbf{v}_1$ , whose dynamics are determined by the mode's energy dissipation rate  $\Gamma_m = 2\pi f_m/Q_m$  where  $Q_m$  is the mechanical quality factor. Fitting these peaks with a thermomechanical noise spectrum [47] we find  $Q_m = 7.5 \times 10^4$  and  $5.8 \times 10^5$  at 300K and 5K, respectively. Note that in the studies presented here, the fiber taper input power is sufficiently low to ensure that it does not affect the nanobeam dynamics; it functions only as a displacement sensor.

Turning on the microscope field introduces optomechanical back action that can be analyzed using the simplified geometry in Fig. 1(c). The local field intensity  $I$  in the nanobeam due to the microscope depends on both the nanobeam's height above the substrate,  $z_s$ , and its distance to the microscope focal plane,  $z_f$ , and can be approximated as  $I = I_f(z_f)\chi(z_s)$ . Here  $I_f$  describes the  $z_f$  dependent microscope field intensity, and the etalon

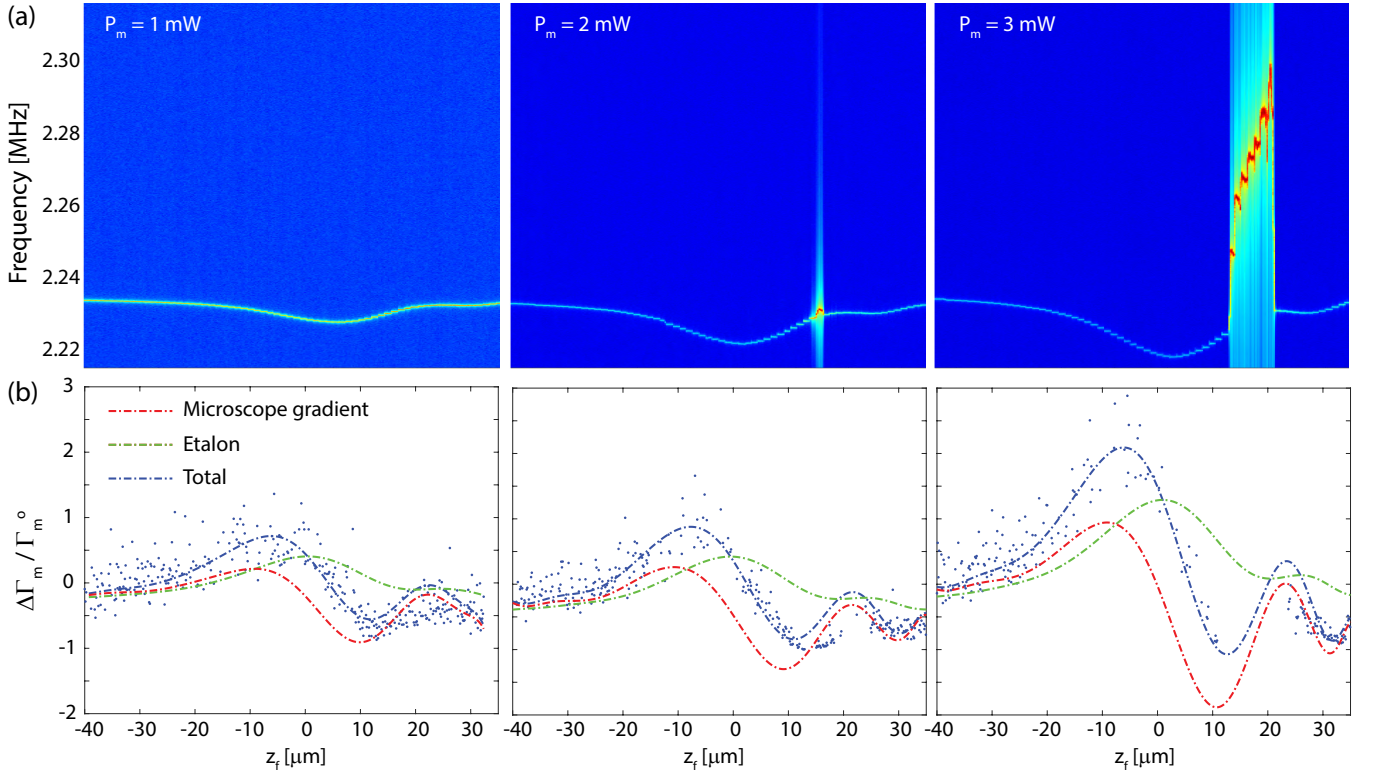


FIG. 2. Nanobeam-microscope optomechanics at room temperature: (a) Spectrograph showing the power spectral density of the fiber taper transmission near the  $\mathbf{v}_1$  nanobeam mode frequency as a function of microscope focus height, for varying microscope green laser power. The sample is at room temperature. Negative values of  $z_f$  indicate that the focal position is below the nanobeam. (b) Optomechanical damping of diamond nanobeam  $\mathbf{v}_1$  mode, normalized by its intrinsic dissipation rate, as a function of microscope focal height and varying microscope power. Fits are from the model in Eq. (1) input with a normalized  $I(z_f)$  profile derived from  $\Delta f_m$ . Contributions from the etalon and microscope gradient terms in Eq. (2) are also shown.

enhancement factor  $\chi(z_s)$  describes the influence of interference between reflections from the substrate with the incident field. Note that in this simplified model  $I_f(z_f)$  implicitly accounts for geometry related local field corrections, and that we have assumed that changes in  $z_s$  due to nanobeam motion are sufficiently small that the etalon contribution can be treated as a separable scaling factor; this representation becomes convenient later for analyzing etalon and microscope related contributions to the intensity gradient. Vertical displacement  $dz$  of the nanobeam due to optical forces from  $I$  modifies  $z_s$  and  $z_f$  by  $\pm dz$ , respectively, which in turn changes  $I$ . This optomechanical feedback, when combined with a lag between the nanobeam position and  $I$ , can amplify or damp mechanical motion. Lateral nanobeam displacement,  $dx$ , also modifies  $I$  and can create back action; it is omitted here for clarity but is discussed later in this letter.

For the microscope illuminated diamond nanobeam, the dominant optical forces were found to be photother-

mal, and the optomechanical damping  $\Delta\Gamma_m$  is given by

$$\frac{\Delta\Gamma_m(z_f)}{\Gamma_m^o} = Q_m^o \frac{2\pi f_m^o \tau}{1 + (2\pi f_m(z_f)\tau)^2} \mathcal{G} \frac{dI(z_f)}{dz} \sigma, \quad (1)$$

where  $\sigma$  is the nanobeam optical power absorption cross-section, and  $\Gamma_m^o$  and  $Q_m^o$  are intrinsic values in absence of the microscope field [35, 41]. The nanobeam's deflection amplitude for a given absorbed power  $\sigma I$  is determined by photothermal coupling coefficient  $\mathcal{G}$  (units of m/W), and depends on the nanobeam's geometry, internal compressive stress, and the presence of pre-buckling [44]. While the titanium layer increases  $\sigma$ , it was not found to be necessary to observe photothermal self-oscillations in these nanobeams [44]. Note that a non-instantaneous thermal response time  $\tau$  is required to realize optomechanical heating or cooling. Finite element (COMSOL) simulations predict  $2\pi f_m \tau \sim 3$ , taking into account the reduced thermal conductivity of nanostructured diamond [48].

The gradient of the microscope field profile  $I_f$  was found to play a critical role in determining whether  $dI/dz$ , and as a result  $\Delta\Gamma_m$ , is positive or negative, i.e.

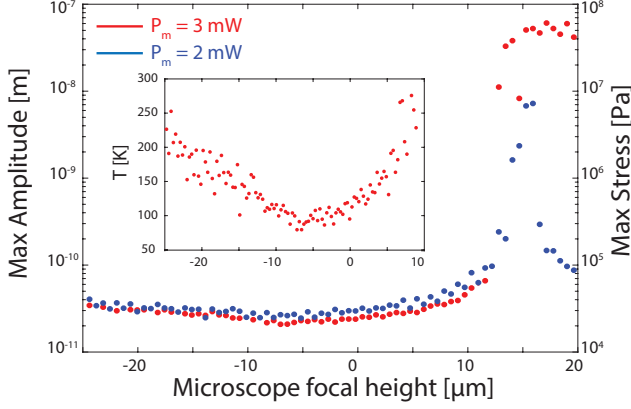


FIG. 3. Amplitude (left axis) and maximum internal dynamic stress (right axis) of the  $v_1$  mode at room temperature as a function of microscope focal plane height for 2 mW and 3 mW microscope power. The sample is at room temperature. When the nanobeam self oscillates, maximum stress just below  $\sim 100$  MPa near the nanobeam clamping points can be realized. Inset: Effective normal mode temperature for 3 mW microscope power as a function of microscope height scanning through the regime of maximum damping.

whether the optomechanical back action damps or amplifies the nanobeam motion. This is in contrast to cavity optomechanical systems, where back action is dominated by  $\chi$  and whose sign is independent of the external coupling optics. To study the optomechanical back action of the microscope field, the objective was aligned with the centre of the nanobeam, and scanned vertically (1  $\mu\text{m}$  steps, 2.9 s/step) while continuously monitoring  $S_{vv}$ . Figure 2(a), shows room temperature result of this measurement for microscope laser powers  $P_m = 1, 2$  and 3 mW. The mechanical frequency  $f_m(z_f) = f_m^o + \Delta f_m(z_f)$  is observed to decrease from its intrinsic value  $f_m^o$  as the microscope field is focused on the nanobeam. The profile shows a smooth change in the frequency reminiscent of the laser intensity in the  $z$  direction, and its sign is consistent with optical absorption and heating of a compressively stressed nanobeam [44]. It provides a means for directly measuring the  $z_f$  dependence of  $I_f$ , allowing the measured data to be compared with models in Eq. (1), as discussed in detail below. In general,  $\Delta f_m$  is also affected by dynamic photothermal, as well as dynamic and static optical gradient force effects [44]. These effects are predicted to be much smaller than the maximum observed  $|\Delta f_m|$  and are not considered here.

The impact of the microscope intensity gradient on the nanobeam dynamics is revealed by a broadening of the resonance when the objective is focused above the nanobeam, and a narrowing when the objective is focused below the nanobeam. This is most dramatically seen near  $z_f = 15 \mu\text{m}$  in the  $P_m = 2$  and 3 mW measurements in Fig. 2(a), where the peak value of  $S_{vv}$  increases

by orders of magnitude. This is accompanied by a dramatic stiffening in  $f_m$  resulting from nonlinear nanomechanical effects in the compressively stressed nanobeam [44]. To analyze the nanobeam dynamics quantitatively,  $\Delta \Gamma_m(z_f)$  was extracted from fits to  $S_{vv}(f; z_f)$ , as shown in Fig. 2(b). These plots show that the nanobeam's mechanical motion is either damped ( $\Delta \Gamma_m > 0$ ) or amplified ( $\Delta \Gamma_m < 0$ ) depending on where the microscope is focused. Notably, the sign of  $\Delta \Gamma_m$  changes as the focus is scanned from above to below the nanobeam. Near  $z_f = 15 \mu\text{m}$ , we find that  $\Gamma_m \sim 0$  ( $\Delta \Gamma_m = -\Gamma_m^o$ ), indicative of the nanobeam entering a regime of self-oscillation, in agreement with the increase in the  $S_{vv}$  peak amplitude observed in Fig. 2(a) for  $P_m = 2$  mW and 3 mW.

This behaviour illustrates a key feature of our system: the dependence of the sign of  $\Delta \Gamma_m(z_f)$  on the microscope intensity gradient. By fitting the data in Figs. 2(b) with the model from Eq. (1), the relative contributions from the etalon and microscope back action were predicted. This was achieved by expanding the microscope intensity gradient,

$$\frac{dI}{dz} = -\chi \left( \frac{dI_f(z_f)}{dz_f} - I_f(z_f) \frac{1}{\chi} \frac{d\chi}{dz_s} \right), \quad (2)$$

inferring  $dI_f/dz_f$  and  $I_f(z_f)$  from  $\Delta f_m(z_f)$  to within a proportionality constant, and fitting Eq. (1) to the data. In addition to  $f_m$  and  $\Gamma_m$ , this fit requires two free parameters: an overall scaling factor and a factor related to  $\chi$  that determines the relative contributions in Eq. (2) of the first microscope intensity gradient term and the second etalon term. Contributions from these two terms to  $\Delta \Gamma_m$  are shown in Fig. 2(b), where we see that the etalon term tends to damp the mechanical vibrations in our experiment, and has the effect of shifting the zero of  $\Delta \Gamma_m(z_f)$ . Note that the asymmetry and oscillations in  $\Delta f_m$  that are uncharacteristic of an ideal Gaussian microscope field are related to aberrations from the cryostat window [49].

The amplification and damping of the nanobeam motion is further analyzed in Fig. 3, which plots the measured RMS nanobeam displacement amplitude deduced from  $S_{vv}$ , for varying  $z_f$  and  $P_m$ . The amplitude is extracted from the area under  $S_{vv}$ , normalized with respect to the thermomechanical vibration amplitude squared in absence of the microscope field [50]. When  $P_m = 3$  mW, the self-oscillation amplitude reaches close to 100 nm, which is three orders of magnitude greater than the nanobeam's intrinsic thermal motion. In contrast, when the microscope position is set to  $z_f \sim -5 \mu\text{m}$ , the thermal motion of the nanobeam is damped, effectively cooling the nanobeam resonance to a temperature  $T_{\text{eff}} \sim 80$  K from the ambient sample temperature  $T_s = 300$  K, as shown in the inset to Fig. 3. This inference of temperature from resonance area was found to be consistent with  $T_{\text{eff}} = T_s / (1 + \Delta \Gamma_m / \Gamma_m^o)$  predicted from the measured  $\Delta \Gamma_m$  in Fig. 2(b) [20].

The effect of the optomechanical back action can be enhanced by pre-cooling the sample to cryogenic conditions, which reduces the intrinsic mechanical dissipation [51], in turn increasing  $|\Delta\Gamma_m/\Gamma_m^o|$ , as shown in Eq. (1), which corresponds a reduction in the optical power required to excite self-oscillations or to optomechanically cool the sample to a given temperature. This is illustrated in Figs. 4(a) and 4(b), which shows  $S_{vv}$  and the RMS amplitude inferred from the area under  $S_{vv}$  for varying  $z_f$ , respectively, when the sample is cooled to 5 K. At this temperature,  $Q_m^o$  increases by an order of magnitude as shown in Fig. 1(b), and self-oscillation is observed in both measurements, which were performed at  $P_m = 150 \mu\text{W}$  and  $P_m = 60 \mu\text{W}$ , respectively. These self-oscillations have an amplitude comparable to those excited by orders of magnitude larger  $P_m$  at room temperature.

The nanobeam's higher  $Q_m^o$  at cryogenic temperature also enables excitation of in-plane nanobeam motion. This is shown in Fig. 4(b), which plots  $S_{vv}$  near  $f_m = 3.0 \text{ MHz}$  of the in-plane  $\mathbf{h}_1$  mode as a function of lateral ( $x$ ) displacement of the objective for  $P_m = 450 \mu\text{W}$ . Note that the  $\sim 4 \mu\text{m}$   $x$  scan length is much smaller than the  $z$  scan lengths discussed above owing to the tighter lateral focus of the microscope field compared to its depth of focus. Self-oscillations near  $x = 0.75 \mu\text{m}$  are evident, and the sign of the observed back action is asymmetric relative to  $x$ , indicating that heating the nanobeam causes it to deflect laterally in a fixed direction independent of the precise position of the focused spot, possibly due to an asymmetry in its fabricated geometry.

A tantalizing prospect is taking advantage of the higher  $Q_m^o$  at cryogenic temperature for enhanced optomechanical cooling of the nanomechanical resonator:  $T_{\text{eff}}$  far below 1 K is naively expected to be achievable at low  $T_s$  for the  $\Delta\Gamma_m$  measured at mW power levels in Fig. 2(b). However, at  $T_s = 5 \text{ K}$  the specific heat of diamond is four orders of magnitude smaller than at room temperature, as it follows a  $T_s^3$  relation for temperatures far below diamond's Deybe temperature of 2200 K. As a result, at high  $P_m$  required for maximum optomechanical cooling, absorbed optical power easily heats the nanobeam, counteracting the optomechanical damping. This competition between optomechanical cooling and absorptive heating is illustrated by the measurements in Fig. 4(d), which compares  $S_{vv}$  of the  $\mathbf{v}_1$  mode with and without the 3 mW green laser incident on the cryogenically cooled nanobeam. With the focus optimized to maximize optomechanical damping,  $Q_m \sim 3340$  was observed, suggesting a reduction in  $T_{\text{eff}}$  of over two orders of magnitude. However, the area under  $S_{vv}$  was reduced by a much more modest factor of 2.4, corresponding to  $T_{\text{eff}} = 2.2 \text{ K}$ , indicating that optical absorption is increasing  $T_s$ .

Spectral diffusion of  $f_m$  related to, for example, low frequency movement of the microscope focus due to cryo-

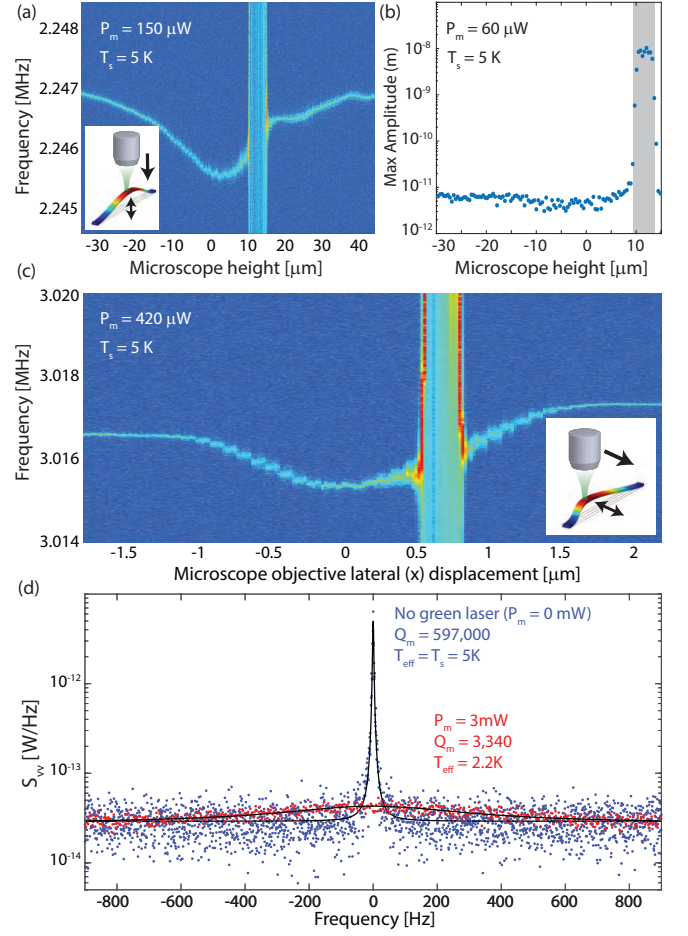


FIG. 4. Nanobeam-microscope optomechanics at cryogenic temperature: (a) Spectrograph and (b) oscillation amplitude of the  $\mathbf{v}_1$  nanobeam mode motion for varying focal plane height, detected via fiber taper transmission. (c) Spectrograph of the in-plane  $\mathbf{h}_1$  nanobeam mode, for varying lateral position ( $x$ ) of the microscope objective. (d) Power spectral density of the fiber taper transmission detected  $\mathbf{v}_1$  mode motion with the microscope off ( $P_m = 0 \text{ mW}$ ) and on ( $P_m = 3 \text{ mW}$ ) with  $z_f$  optimized to maximize  $\Delta\Gamma_m$ .

stat pump vibrations, can also broaden the mechanical resonance. This effect is likely playing a role given that the damped  $Q_m$  at 5 K implies  $\Delta\Gamma_m \sim 2\pi f_m/5000$ , which is much larger than the room temperature measurement of  $\Delta\Gamma_m \sim 2\pi f_m/25000$  in Fig. 2(b). Further evidence of spectral broadening unrelated to dynamic optomechanical back action was observed in the  $x$  scan measurements. At low  $P_m$ , broadening was observed symmetrically when the objective was focused on either side of the nanobeam, where the intensity gradient is maximum and vibrations in  $x$  due to sample or microscope movement result in fluctuations in absorbed power and  $f_m$ , and was minimized when  $x = 0$ . In contrast, at higher  $P_m$  self-oscillations were observed with the focus on the  $x > 0$  side of the nanobeam, as discussed above. Finally,

note that spectral diffusion does not affect the area under  $S_{vv}$  and the resulting inferred  $T_{\text{eff}}$  [52], and that the agreement at room temperature between  $T_{\text{eff}}$  extracted from the area and linewidth of  $S_{vv}$  indicates that both spectral broadening and sample heating is specific to the cryogenic measurements reported here.

The potential for application of these results to the field of spin-optomechanics and phonon-photon-spin coupling is significant. The microscope field is generated using a confocal microscope commonly used for spectroscopy of diamond NV color centers, making this approach particularly suited to coupling electron spins of these systems to phonons. Such coupling would allow optomechanical control of color center spins, building on previous work reliant on piezo actuation [22]. For the self-oscillation amplitudes observed in the work reported here, dynamic stress field in the 100 MPa range are expected, as predicted from COMSOL and shown in Fig. 3. This corresponds to a predicted spin-phonon coupling rate  $G_g/2\pi \sim 1$  MHz and  $G_e/2\pi \sim 100$  THz, for the ground state and excited state, respectively, of a negatively charged NV centre, which is comparable the stress fields used in recent demonstrations of NV stress manipulation [24–26]. The resulting optomechanical spin control could provide a path towards creating a transducer [30, 33] for coupling photons to spins without relying on direct optical transitions of the color centre, enabling interfacing telecommunication photons used in quantum networks to diamond quantum memories.

In conclusion, we have demonstrated optomechanical amplification and damping of diamond nanomechanical resonators into using a microscope field, while simultaneously optomechanically detecting the resonator motion using an external waveguide. To the best of our knowledge, this is the first demonstration of tunable optomechanical damping and amplification of a nanomechanical resonator without using a cavity or etalon resonance. Using this tunability to maximize optomechanical damping, we have shown that cooling of the nanobeam’s fundamental normal mode from room temperature to below 80K is possible. The potential to extend this cooling to lower effective temperature was demonstrated by measurements at low temperature, where  $Q_m$  is increased and the impact of the optomechanical coupling on the nanobeam dynamics is enhanced. This is particularly promising in light of recent progress in enhancing  $Q_m$  of nanomechanical resonators through soft-clamping [53] and phononic crystal designs.

**Acknowledgments:** Thank you to Aaron Hryciw, J.P. Hadden and M. Mitchell for assistance. This work was supported by NSERC (Discovery and Research Tools and Instruments), CFI, AITF and NRC.

\* These authors contributed equally. Current address of HJ: Department of Physics, CUNY-City College of New York, New York, NY 10031, USA, hjayakumar@ccny.cuny.edu

† pbarclay@ucalgary.ca

- [1] A. Ashkin, “Acceleration and trapping of particles by radiation pressure,” *Phys. Rev. Lett.* **24**, 156–159 (1970).
- [2] LIGO Scientific, BP Abbott, R Abbott, TD Abbott, F Acernese, K Ackley, C Adams, T Adams, P Addesso, RX Adhikari, *et al.*, “Gw170104: observation of a 50-solar-mass binary black hole coalescence at redshift 0.2,” *Physical Review Letters* **118**, 221101 (2017).
- [3] Simon Gröblacher, Klemens Hammerer, Michael R Vanner, and Markus Aspelmeyer, “Observation of strong coupling between a micromechanical resonator and an optical cavity field,” *Nature* **460**, 724–727 (2009).
- [4] Jasper Chan, T. P. Mayer Alegre, Amir H. Safavi-Naeini, Jeff T. Hill, Alex Krause, Simon Gröblacher, Markus Aspelmeyer, and Oskar Painter, “Laser cooling of a nanomechanical oscillator into its quantum ground state,” *Nature* **478**, 89–92 (2011).
- [5] Justin D Cohen, Seán M Meenehan, Gregory S MacCabe, Simon Gröblacher, Amir H Safavi-Naeini, Francesco Marsili, Matthew D Shaw, and Oskar Painter, “Phonon counting and intensity interferometry of a nanomechanical resonator,” *Nature* **520**, 522–525 (2015).
- [6] Ralf Riedinger, Sungkun Hong, Richard A Norte, Joshua A Slater, Juying Shang, Alexander G Krause, Vikas Anant, Markus Aspelmeyer, and Simon Gröblacher, “Non-classical correlations between single photons and phonons from a mechanical oscillator,” *Nature* **530**, 313–316 (2016).
- [7] V. Sudhir, R. Schilling, S. A. Fedorov, H. Schütz, D. J. Wilson, and T. J. Kippenberg, “Quantum correlations of light from a room-temperature mechanical oscillator,” *Phys. Rev. X* **7**, 031055 (2017).
- [8] T. P. Purdy, K. E. Grutter, K. Srinivasan, and J. M. Taylor, “Quantum correlations from a room-temperature optomechanical cavity,” *Science* **356**, 1265–1268 (2017).
- [9] Ralf Riedinger, Andreas Wallucks, Igor Marinković, Clemens Löschnauer, Markus Aspelmeyer, Sungkun Hong, and Simon Gröblacher, “Remote quantum entanglement between two micromechanical oscillators,” *Nature* **556**, 473 (2018).
- [10] G. Anetsberger, E. Gavartin, O. Arcizet, Q.P. Unterreithmeier, E.M. Weig, M.L. Gorodetsky, J.P. Kotthaus, and T.J. Kippenberg, “Measuring nanomechanical motion with an imprecision below standard quantum limit,” *Phys. Rev. A* **82**, 061804 (2010).
- [11] E. Gavartin, P. Verlot, and T.J. Kippenberg, “A hybrid on-chip optomechanical transducer for ultrasensitive force measurements,” *Nature Nanotech.* **7**, 509–514 (2012).
- [12] S. Forstner, S. Prams, J. Knittel, ED van Ooijen, JD Swaim, GI Harris, A. Szorkovszky, WP Bowen, and H. Rubinsztein-Dunlop, “Cavity optomechanical magnetometer,” *Phys. Rev. Lett.* **108**, 120801 (2012).
- [13] Marcelo Wu, Nathanael L-Y Wu, Tayyaba Firdous, Fatemeh Fani Sani, Joseph E Losby, Mark R Freeman, and Paul E Barclay, “Nanocavity optomechanical torque magnetometry and radiofrequency susceptometry,” *Nature*

- ture Nanotechnology **12**, 127–131 (2017).
- [14] Amir H Safavi-Naeini, TP Mayer Alegre, Jasper Chan, Matt Eichenfield, Martin Winger, Qiang Lin, Jeffrey T Hill, DE Chang, and Oskar Painter, “Electromagnetically induced transparency and slow light with optomechanics,” *Nature* **472**, 69–73 (2011).
  - [15] Stefan Weis, Rémi Rivière, Samuel Deléglise, Emanuel Gavartin, Olivier Arcizet, Albert Schliesser, and Tobias J Kippenberg, “Optomechanically induced transparency,” *Science* **330**, 1520–1523 (2010).
  - [16] Chunhua Dong, Victor Fiore, Mark C Kuzyk, and Hailin Wang, “Optomechanical dark mode,” *Science* **338**, 1609–1613 (2012).
  - [17] Yuxiang Liu, Marcelo Davanço, Vladimir Aksyuk, and Kartik Srinivasan, “Electromagnetically induced transparency and wideband wavelength conversion in silicon nitride microdisk optomechanical resonators,” *Phys. Rev. Lett.* **110**, 223603 (2013).
  - [18] David P Lake, Matthew Mitchell, Yasmeen Kamaliddin, and Paul E Barclay, “Optomechanically induced transparency and cooling in thermally stable diamond microcavities,” *ACS Photonics* **5**, 782 (2018).
  - [19] T.J. Kippenberg and K.J. Vahala, “Cavity optomechanics: Back-action at the mesoscale,” *Science* **321**, 1172–1176 (2008).
  - [20] Markus Aspelmeyer, Tobias J. Kippenberg, and Florian Marquardt, “Cavity optomechanics,” *Rev. Mod. Phys.* **86**, 1391–1452 (2014).
  - [21] Igor Aharonovich, Andrew D. Greentree, and Steven Praver, “Diamond photonics,” *Nature Photon.* **5**, 397–405 (2011).
  - [22] Donghun Lee, Kenneth W Lee, Jeffrey V Cady, Preeti Ovartchaiyapong, and Ania C Bleszynski Jayich, “Topical review: spins and mechanics in diamond,” *Journal of Optics* **19**, 033001 (2017).
  - [23] E. R. MacQuarrie, T. A. Gosavi, N. R. Jungwirth, S. A. Bhave, and G. D. Fuchs, “Mechanical spin control of nitrogen-vacancy centers in diamond,” *Phys. Rev. Lett.* **111**, 227602 (2013).
  - [24] P. Ovartchaiyapong, K. W. Lee, B. A. Myers, and A. C. Bleszynski Jayich, “Dynamic strain-mediated coupling of a single diamond spin to a mechanical resonator,” *Nat. Commun.* **5**, 4429 (2014).
  - [25] J. Teissier, A. Barfuss, P. Appel, E. Neu, and P. Maletinsky, “Strain coupling of a nitrogen-vacancy center spin to a diamond mechanical oscillator,” *Phys. Rev. Lett.* **113**, 020503 (2014).
  - [26] A. Barfuss, J. Teissier, E. Neu, A. Nunnenkamp, and P. Maletinsky, “Strong mechanical driving of a single electron spin,” *Nature Phys.* **11**, 820–824 (2015).
  - [27] E. R. MacQuarrie, T. A. Gosavi, A. M. Moehle, N. R. Jungwirth, S. A. Bhave, and G. D. Fuchs, “Coherent control of a nitrogen-vacancy center spin ensemble with a diamond mechanical resonator,” *Optica* **2**, 233–238 (2015).
  - [28] Srujan Meesala, Young-Ik Sohn, Haig A. Atikian, Samuel Kim, Michael J. Burek, Jennifer T. Choy, and Marko Lončar, “Enhanced strain coupling of nitrogen-vacancy spins to nanoscale diamond cantilevers,” *Phys. Rev. Applied* **5**, 034010 (2016).
  - [29] D. Andrew Golter, Thein Oo, Mayra Amezcua, Ignas Lekavicius, Kevin A. Stewart, and Hailin Wang, “Coupling a surface acoustic wave to an electron spin in diamond via a dark state,” *Phys. Rev. X* **6**, 041060 (2016).
  - [30] D. Andrew Golter, Thein Oo, Mayra Amezcua, Kevin A. Stewart, and Hailin Wang, “Optomechanical quantum control of a nitrogen-vacancy center in diamond,” *Phys. Rev. Lett.* **116**, 143602 (2016).
  - [31] M.-A. Lemonde, S. Meesala, A. Sipahigil, M. J. A. Schuetz, M. D. Lukin, M. Loncar, and P. Rabl, “Phonon networks with silicon-vacancy centers in diamond waveguides,” *Phys. Rev. Lett.* **120**, 213603 (2018).
  - [32] Mark C Kuzyk and Hailin Wang, “Phononic quantum networks of solid-state spins with alternating and frequency-selective waveguides,” *arXiv preprint arXiv:1804.07862* (2018).
  - [33] M. J. A. Schuetz, E. M. Kessler, G. Giedke, L. M. K. Vandersypen, M. D. Lukin, and J. I. Cirac, “Universal quantum transducers based on surface acoustic waves,” *Phys. Rev. X* **5**, 031031 (2015).
  - [34] D. Rugar and P. Grütter, “Mechanical parametric amplification and thermomechanical noise squeezing,” *Phys. Rev. Lett.* **67**, 699–702 (1991).
  - [35] Robert A Barton, Isaac R Storch, Vivekananda P Adiga, Reyu Sakakibara, Benjamin R Cipriany, B Ilic, Si Ping Wang, Peijie Ong, Paul L McEuen, Jeevak M Parpia, *et al.*, “Photothermal self-oscillation and laser cooling of graphene optomechanical systems,” *Nano Lett.* **12**, 4681–4686 (2012).
  - [36] Z. Yie, K. Turner, N.J. Miller, and S. Shaw, “Sensitivity enhancement using parametric amplification in a resonant sensing array,” in *Proceedings of the 13th Hilton Head Solid State Sensors and Actuators Conference* (2010).
  - [37] Qiang Lin, Jessie Rosenberg, Xiaoshun Jiang, Kerry J. Vahala, and Oskar Painter, “Mechanical oscillation and cooling actuated by the optical gradient force,” *Phys. Rev. Lett.* **103**, 103601 (2009).
  - [38] O. Arcizet, P. F. Cohadon, T. Briant, M. Pinard, and A. Heidmann, “Radiation-pressure cooling and optomechanical instability of a micromirror,” *Nature* **444**, 71–74 (2006).
  - [39] S. Gigan, H. R. Böhm, M. Paternostro, F. Blaser, G. Langer, J. B. Hertzberg, K. C. Schwab, D. Bäuerle, M. Aspelmeyer, and A. Zeilinger, “Self-cooling of a micromirror by radiation pressure,” *Nature* **444**, 67–70 (2006), [arXiv:quant-ph/0607068](https://arxiv.org/abs/quant-ph/0607068).
  - [40] Constanze Metzger, Ivan Favero, Alexander Ortlieb, and Khaled Karrai, “Optical self cooling of a deformable fabry-perot cavity in the classical limit,” *Phys. Rev. B* **78**, 035309 (2008).
  - [41] C. H. Metzger and K. Karrai, “Cavity cooling of a microlever,” *Nature* **432**, 1002–1005 (2004).
  - [42] I. Favero, C. Metzger, S. Camerer, D. König, H. Lorenz, J. P. Kotthaus, and K. Karrai, “Optical cooling of a micromirror of wavelength size,” *Appl. Phys. Lett.* **90**, 104101 (2007).
  - [43] Daniel Ramos, Eduardo Gil-Santos, Valerio Pini, Jose M. Llorens, Marta Fernandez-Regulez, Alvaro San Paulo, M. Calleja, and J. Tamayo, “Optomechanics with silicon nanowires by harnessing confined electromagnetic modes,” *Nano Letters* **12**, 932–937 (2012), PMID: 22268657, <http://dx.doi.org/10.1021/nl204002u>.
  - [44] Behzad Khanaliloo, Harishankar Jayakumar, Aaron C. Hryciw, David P. Lake, Hamidreza Kaviani, and Paul E. Barclay, “Single-crystal diamond nanobeam waveguide optomechanics,” *Phys. Rev. X* **5**, 041051 (2015).
  - [45] M Poggio, CL Degen, HJ Mamin, and D Rugar, “Feed-

- back cooling of a cantilevers fundamental mode below 5 mk,” *Physical Review Letters* **99**, 017201 (2007).
- [46] Chris P. Michael, Matthew Borselli, Thomas J. Johnson, Colin Chrystala, and Oskar Painter, “An optical fiber-taper probe for wafer-scale microphotonic device characterization,” *Opt. Express* **15**, 4745–4752 (2007).
  - [47] A.N. Cleland and M.L. Roukes, “Noise processes in nanomechanical resonators,” *J. Appl. Phys.* **92**, 2758 (2002).
  - [48] Wu Li, Natalio Mingo, L. Lindsay, D. A. Broido, D. A. Stewart, and N. A. Katcho, “Thermal conductivity of diamond nanowires from first principles,” *Phys. Rev. B* **85**, 195436 (2012).
  - [49] Michael J Nasse and Jörg C Woehl, “Realistic modeling of the illumination point spread function in confocal scanning optical microscopy,” *Josa a* **27**, 295–302 (2010).
  - [50] Matthew Mitchell, Behzad Khanaliloo, David P. Lake, Tamiko Masuda, J. P. Hadden, and Paul E. Barclay, “Single-crystal diamond low-dissipation cavity optomechanics,” *Optica* **3**, 963–970 (2016).
  - [51] Y. Tao, J. M. Boss, B. A. Moores, and C. L. Degen, “Single-crystal diamond nanomechanical resonators with quality factors exceeding one million,” *Nat. Commun.* **5**, 3638 (2013).
  - [52] Joel Moser, Alexander Eichler, Johannes Güttinger, Mark I Dykman, and Adrian Bachtold, “Nanotube mechanical resonators with quality factors of up to 5 million,” *Nature nanotechnology* **9**, 1007 (2014).
  - [53] AH Ghadimi, SA Fedorov, NJ Engelsen, MJ Bereyhi, R Schilling, DJ Wilson, and TJ Kippenberg, “Elastic strain engineering for ultralow mechanical dissipation,” *Science* **360**, 764–768 (2018).